

Experimental design study of nickel removal from aqueous solution by activated carbon and its pore size distribution modification using carbon dioxide gasification for enhancing adsorption efficiency

Mohammad Ali Ale Ebrahim^{a,*}, Taghi Ebadi^b

^aCivil Engineering Department, Sharif University of Technology, Tehran 11365-9313, Iran, Tel. +9821 66164698; Fax: +9821 66414213; email: m.alebrahim@aut.ac.ir (M. Ali Ale Ebrahim)

^bCivil Engineering Department, Amirkabir University, Tehran 15875-4413, Iran, Tel. +9821 64543031; email: tebadi@aut.ac.ir (T. Ebadi)

Received 17 December 2019; Accepted 10 July 2020

ABSTRACT

In this work, nickel removal by a coal-based activated carbon was investigated using response surface methodology. The effects of concentration, pH, and carbon/liquid ratio were considered and optimum conditions were determined. One of the optimum cases was predicted as 73.0% Ni removal efficiency, while its validation test result was 73.3%. Also, the kinetics and equilibrium for Ni removal via activated carbon were determined in a batch system. The parameters of pseudo-second-order kinetic and Freundlich thermodynamic models were determined. As the best nickel removal efficiency was only 73%, modification of the pore size distribution of activated carbon through carbon dioxide gasification at 900°C was accomplished for enhancing the Ni adsorption. Nickel removal by this modified carbon in the optimum condition was improved from 73.3% to 96.1%. Thus, the experimental importance of this work is a 31.1% enhancement in Ni removal efficiency after modification using CO₂ gasification. Finally, the regeneration of spent carbon was performed successfully by acid washing and electro-kinetic methods.

Keywords: Nickel elimination; Response surface methodology; Activated carbon; Pore size distribution improvement; Gasification by carbon dioxide

1. Introduction

One of the most important requirements for human life is high-quality potable water. Meanwhile, toxic heavy metal ions are the main problem in water pollution. Some examples of heavy metals include mercury, cadmium, lead, chromium, cobalt, iron, zinc, and nickel [1]. Nickel exists in some industrial wastewaters such as metal-finishing, textiles, and battery manufacturing [2]. The maximum allowable limit of Ni-based on the environmental standard in drinking water is 0.1 mg/L [3].

The conventional process for heavy metal removal is adsorption by a suitable adsorbent such as activated carbon

due to its low fixed costs [4]. There have been extensive studies on heavy metal removal by activated carbon in the literature. Some examples are adsorption of Fe [5], Cd [6], Pb [7,8], Cu [9], Zn [10], and Cr [11,12].

Although various activated carbons from different sources such as from rubber tires [13], pine needles [14], olive stone [15], walnut and hazelnut shells [9], almond husk [16], barley straw ash [17], dried biomass [18], date stone [19], silica-activated carbon composites [20], and activated carbon cloths [21] have been tested to remove Ni from water, the coal-based activated carbon is the most typical sorbent [4]. However, removal efficiencies of Ni by conventional

* Corresponding author.

activated carbons may not be high enough due to inappropriate pore size distribution (PSD) of the commercial activated carbon. Since Ni^{2+} is a relatively large ion, the proportion of mesopores should be increased vs. micropores in the PSD of activated carbon for higher removal efficiencies. As evidence, it was reported that the maximum Ni removal efficiency of activated carbon was about half of the removal obtained by carbon nanotubes due to the dominance of greater pores in the PSD of carbon nanotubes vs. activated carbon PSD [22]. Meanwhile, it was proved that producing large channels (mesopores) during PSD modification of activated carbon by potassium bromate can improve Ni removal efficiency considerably [23].

Physical and chemical methods have been used for preparing activated carbons from various initial sources. Physical activation by water vapor or carbon dioxide is preferred over chemical activation by reagents such as zinc chloride, potassium hydroxide, and phosphoric acid [24]. There are pyrolysis and physical activation steps in the physical method. In the first step, pyrolysis, the initial source is heated in an inert gas stream up to moderate temperatures to produce a char. Then, in the second step, activation, the producing char reacts with H_2O or CO_2 at higher temperatures to accomplish partial and controlled gasification for producing the final porous and high-surface area activated carbon. The gasification temperature and exposure time are two important parameters determining the internal structure and PSD of the final produced activated carbon [25].

As mentioned, the main drawback of the previous works in the field of Ni removal by activated carbon has been relatively low adsorption efficiency. Thus, PSD modification of activated carbon through CO_2 gasification can improve Ni removal efficiency whose study is the novelty of the present work. In this work, the removal of nickel ion from aqueous solutions by a commercial coal-based activated carbon was explored through the response surface methodology (RSM) experimental design in a batch system. The operating conditions included the nickel concentration, pH, and carbon/water ratio, with the Ni removal efficiencies presented as functions of these operating conditions. Further, the optimum conditions were determined based on RSM. Then, the kinetics and equilibrium equations of nickel removal by activated carbon were expressed based on these experiments. Next, modification of activated carbon through high-temperature gasification with CO_2 was performed for improving the PSD, thus enhancing Ni removal efficiency. Finally, the spent adsorbent was regenerated by acid washing and electro-kinetic methods.

2. Materials and methods

2.1. Raw materials

The activated carbon was purchased from Jacobi, Sweden (Aqua Sorb 2000 type). This adsorbent is a granular (8–30 mesh: 0.6–2.36 mm) coal-based activated carbon for water treatment purposes. The iodine number, ash content, and apparent density of this adsorbent were reported as 950 mg/g, 13%, and 0.49 g/mL, respectively.

The initial and modified activated carbons were characterized in this work using Brunauer–Emmett–Teller (BET)

surface area as well as 55-point N_2 -adsorption PSD tests by Autosorb 1-MP from Quantachrome, (U.S.A.). The BET surface area, Saito-Foley (SF) method micropore volume, and Barrett–Joyner–Halenda (BJH) method mesopore volume of adsorbents were measured by these N_2 -adsorption PSD tests.

Further, scanning electron microscopy (SEM) pictures of adsorbents granules were taken by Philips XL-30 (Netherlands) without grinding them. Also, the pH of the zero charge point was determined by a well-known salt addition method for each adsorbent. Finally, Fourier-transform infrared (FTIR) spectroscopy of the initial and modified activated carbons was determined using Nicolet iS10 (U.S.A.) after grinding them, mixing with KBr powder, and making sample pellets.

2.2. Experimental methodology

2.2.1. Adsorption experimental procedures

Nickel solutions with various Ni concentrations were prepared from the pure nickel nitrate hexahydrate (from ChemLab, Belgium) dissolution in distilled water. All batch-wise adsorption experiments were performed in a 400 mL glass beaker (100 mL solution) with a magnetic stirrer. The solution pH was measured by a digital pH-meter, and pH was controlled within 2–6 by adding a dilute nitric acid solution. At different times, once activated carbon granules and Ni solutions got into contact with each other, the sampling was performed by a small (1 mL) pipette for Ni analysis.

The remaining nickel in the aqueous solution was analyzed by inductively coupled plasma optical emission spectrometry from Varian, U.S.A. (Vista-PRO), with ppb sensitivity.

2.2.2. Kinetic studies

The metal removal after adsorption is expressed as:

$$\text{Metal removal (\%)} = \frac{C_0 - C_e}{C_0} \times 100 \quad (1)$$

where C_0 and C_e represent the initial and final metal concentrations in the solution (mg/L), respectively.

The common kinetic equations for the adsorption process are pseudo-first-order, pseudo-second-order, intraparticle diffusion, and Elovich models. In pseudo-first-order kinetics, it is assumed that the rate of the metal adsorption is proportional to active sites. Meanwhile, in the pseudo-second-order model, the rate of metal adsorption is proportional to the square of active sites. The assumption for the intraparticle diffusion model is that the solute uptake varies with the square-root of adsorption time. Finally, the solid surface of adsorbent is assumed as a heterogeneous structure in the Elovich model [26].

The pseudo-first-order, pseudo-second-order, intraparticle diffusion, and Elovich kinetic equations are presented as follows [27]:

$$\log(q_e - q_t) = \log(q_e) - \frac{k_1}{2.303} t \quad (2)$$

where q_e and q_t represent the adsorption capacities at equilibrium and at any time t (mg/g), and k_1 refers to the rate constant of the pseudo-first-order adsorption (1/min).

$$\frac{t}{q_t} = \frac{1}{k_2 q_e^2} + \frac{t}{q_e} \quad (3)$$

where k_2 is the rate constant of the pseudo-second-order adsorption (g/mg min).

$$q_t = K_{\text{int}} t^{0.5} + C_c \quad (4)$$

where K_{int} is the intraparticle diffusion rate constant (mg/g min^{0.5}).

$$q_t = \frac{1}{\beta} \text{Ln}(\alpha\beta) + \frac{1}{\beta} \text{Ln}(t) \quad (5)$$

where α is the initial rate (mg/g min) and β is the Elovich constant (g/mg).

The kinetic study of nickel ion removal by activated carbon was done in a 50 mg/L Ni aqueous solution, at pH = 6, with 2.5 g carbon per 100 mL of the solution. The sampling time was 15 min up to 90 min, and then 30 min up to 240 min.

2.2.3. Equilibrium studies

The equilibrium magnitude of the adsorbed metal per gram of carbon is:

$$q_e = \frac{(C_0 - C_e)V}{m} \quad (6)$$

where V is the volume of the aqueous phase (L), m denotes the mass of the solid adsorbent (g), and C_0 and C_e represent the initial and final metal concentrations in the solution (mg/L), respectively.

There are various equilibrium models for adsorption including Langmuir, Freundlich, Dubinin–Radushkevich (D–R), and Temkin, which are presented as the following equations [18]:

$$\frac{C_e}{q_e} = \frac{1}{q_m b} + \frac{C_e}{q_m} \quad (7)$$

where q_m is the maximum adsorption capacity (mg/g) and b is the Langmuir constant (L/mg).

$$\text{Ln} q_e = \text{Ln} K_F + \frac{1}{n} \text{Ln} C_e \quad (8)$$

where K_F is the Freundlich constant indicating sorption capacity (mg/g) and n denotes the adsorption intensity.

$$\text{Ln} q_e = \text{Ln} q_s - K_D R^2 T^2 \left[\text{Ln} \left(1 + \frac{1}{C_e} \right) \right]^2 \quad (9)$$

where q_s is the theoretical saturation capacity (mg/g), K_D denotes the D–R constant related to the mean free energy of adsorption (mol²/kJ²), R is the universal gas constant (8.314 J/mol K), and T represents the temperature (K).

$$q_e = \frac{RT}{B_b} \text{Ln}(A_a) + \frac{RT}{B_b} \text{Ln}(C_e) \quad (10)$$

where A_a is the Temkin isotherm constant (L/mg) and B_b is the equilibrium binding constant (J/mol).

Langmuir model assumes equivalent sorption for activation energies. Meanwhile, logarithmic reduction of the activation energy vs. the surface coverage is assumed in the Freundlich equation. Also, the sorption curve is assumed as a function of a solid porous structure in the D–R model. Eventually, the linear reduction of adsorption heat vs. surface coverage is the assumption of the Temkin model [26].

In this work, the equilibrium study of nickel ion removal by activated carbon was performed at pH = 6, 2.5 g carbon per 100 mL solution, 3 h mixing time, as well as 10, 30, 45, and 60 mg/L initial nickel concentrations.

Finally, various adsorption tests were conducted at 28°C, 43°C, and 53°C for the thermodynamic study. Then, the thermodynamic adsorption parameters were evaluated by the van't Hoff equation as follows [28]:

$$\Delta G^\circ = \Delta H^\circ - R\Delta S^\circ = -RT \text{Ln} \left(\frac{mq_e}{VC_e} \right) \quad (11)$$

where ΔG° is standard free energy (kJ/mol), ΔH° and ΔS° represent the enthalpy (kJ/mol) and entropy (J/mol K) of adsorption, respectively. Accordingly, the enthalpy and entropy of adsorption have been determined by the van't Hoff plot.

2.2.4. Experimental design theory

The quantitative effects of operating variables on metal ion removal efficiencies from a solution by activated carbon can be studied using RSM experimental design [29]. This method presents the objective function as a second-order RSM model in terms of independent variables such as [30]:

$$y = \beta_0 + \beta_1 A + \beta_2 B + \beta_3 C + \beta_{11} A^2 + \beta_{22} B^2 + \beta_{33} C^2 + \beta_{12} AB + \beta_{13} AC + \beta_{23} BC \quad (12)$$

where y is the goal function, β_0 denotes a constant, β_1 , β_2 and β_3 represent linear coefficients, β_{12} , β_{13} and β_{23} are interaction coefficients, and β_{11} , β_{22} and β_{33} reflect quadratic coefficients. A , B , and C are coded independent variables including carbon mass/100 mL (A), pH of the solution (B), and initial metal ion concentration (C). Further, each operating parameter is considered at three various levels. In this study, Box–Behnken RSM method was utilized (Design Expert, 7.0.0).

2.2.5. Improving activated carbon by gasification

Generally, physical activation occurs through steam or carbon dioxide. Carbon dioxide (with a lower and controllable gasification rate vs. steam) was used in this study for PSD modification of activated carbon. In this work, activated carbon was modified in a tubular reactor of 5 cm diameter via a carbon dioxide (99.99%) stream. The reactor was inserted in a vertical furnace with a maximum working temperature of 1,200°C and a power of 2 kW for generating high temperatures (Fig. 1). About 100 g of commercial activated carbon was placed in the middle of the reactor and

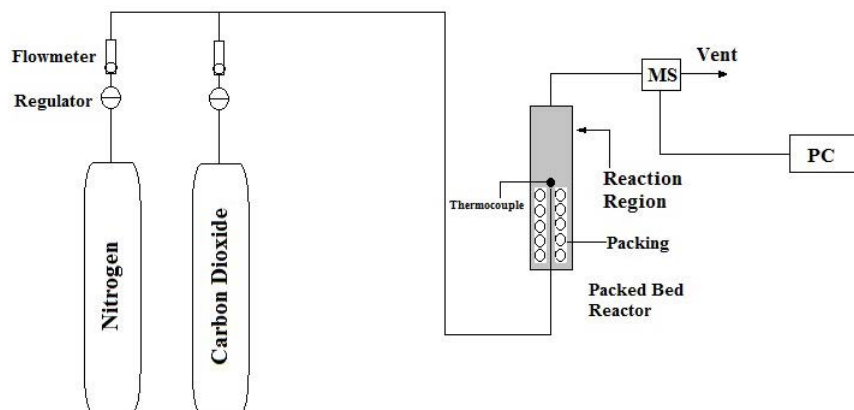


Fig. 1. The setup for modification of activated carbon PSD by CO₂ gasification.

the system was heated to the setpoint under CO₂ stream. Then, after the hold time at an isothermal temperature, the PSD modification was accomplished. The outlet gaseous stream was continuously analyzed via an online mass spectrometer from Leda Mass, (U.K.).

2.2.6. Regeneration procedures

The regeneration tests of the consumed carbons were conducted through sulfuric and nitric acid (from Merck, Germany) washing. The electro-kinetic regeneration experiments were based on 12 V DC and 0.5 A via platinum electrodes on a solution containing the consumed carbons.

In regeneration tests, desorption efficiency can be computed as:

$$D(\%) = 100 \frac{C_d V_d}{C_0 - C_e} \quad (13)$$

where C_d is the metal ion concentration in the desorption solution (mg/L) and V_d is the volume of desorption solution (L).

3. Results and discussion

3.1. Nickel removal kinetics and equilibrium

The SEM pictures (from Philips) of a carbon granule are illustrated in Figs. 2a and b. This figure displays some large pores of the initial carbon, along with bright nickel points on the porous structure following the adsorption test.

Nickel removal efficiencies for the kinetic study are illustrated in Fig. 3a vs. adsorption time. This figure indicates that the appropriate agitation time for further equilibrium tests is about 3 h.

Ni removal kinetic plots are indicated in Figs. 3b–e. Also, Table 1 presents the kinetic constants for nickel removal by activated carbon from various models. According to Table 1, it is seen that the best kinetic equation for Ni removal is the pseudo-second-order model with the highest correlation coefficient. Based on this pseudo-second-order kinetic equation, $q_e = 1.26$ mg/g was estimated for Ni removal by activated carbon.

For equilibrium equations, the plots of various models are shown in Figs. 4a–d and Table 2 for Ni removal by activated carbon. As Fig. 4 indicates, all equilibrium equations are satisfactory. Among them, the Freundlich equation (with

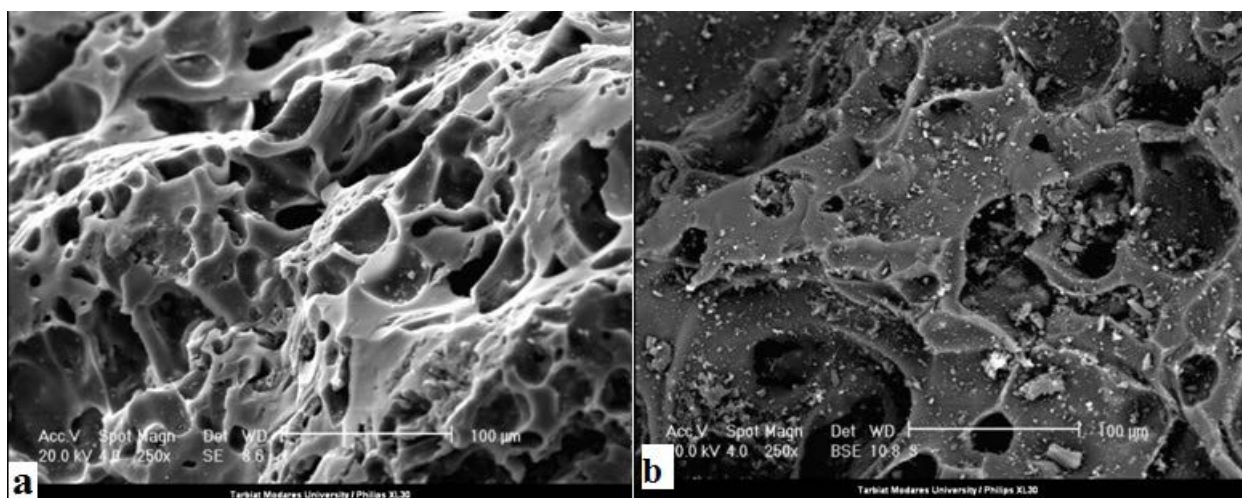


Fig. 2. SEM graphs of initial carbon (a), and this carbon after Ni adsorption (b) with 250× magnification.

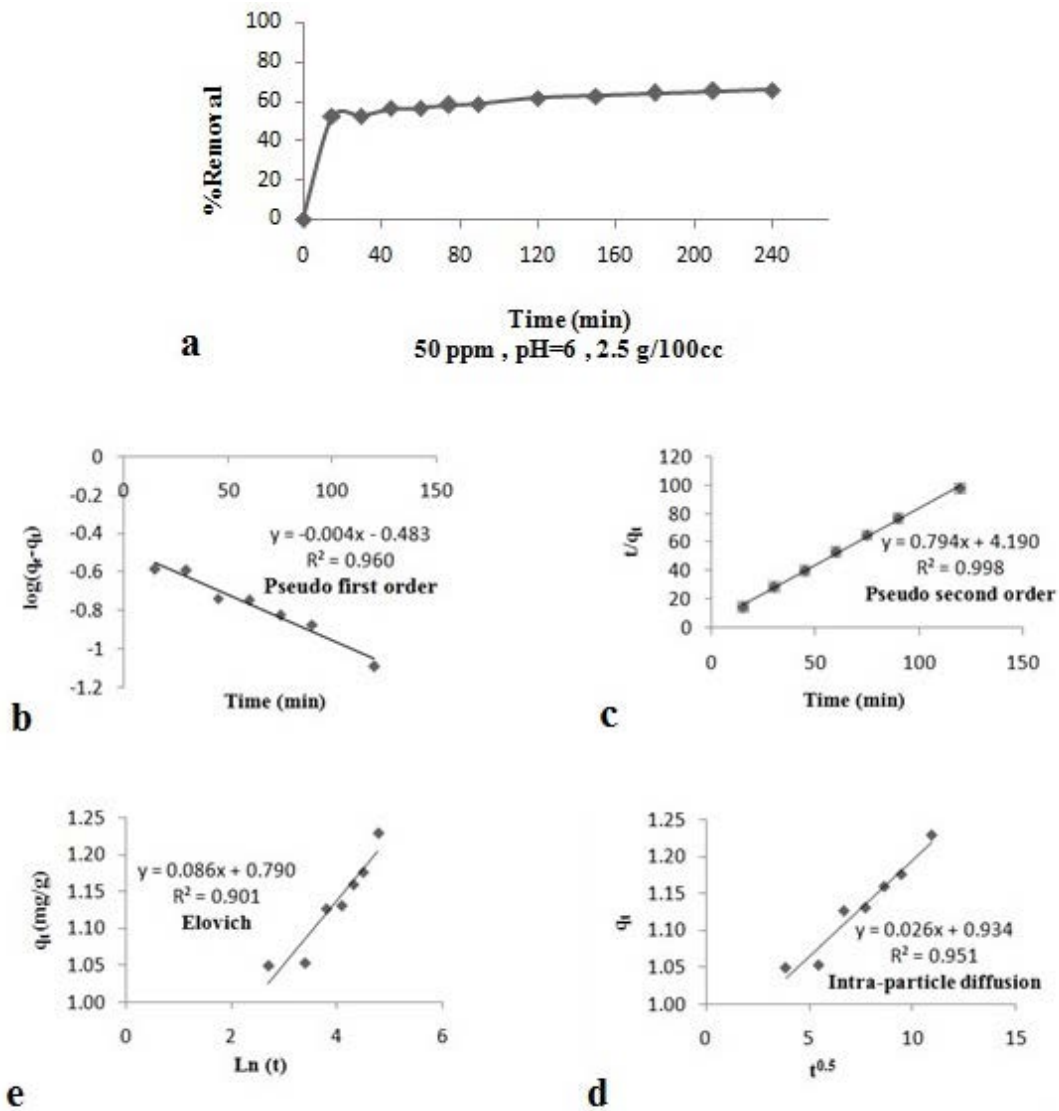


Fig. 3. Ni removal percentages vs. time (a), and the kinetic plots for Ni removal consisting of pseudo-first-order (b), pseudo-second-order (c), intraparticle diffusion (d), and Elovich (e).

$R^2 = 0.998$) is the best for nickel removal equilibrium. In the Freundlich model, n represents the ability for adsorption. The values of n within 0–10 show favorable metal adsorption. Further, since n in Table 2 for nickel removal is 1.272 (near 1.0), the Langmuir-type adsorption is also applicable [26]. In addition, Langmuir and Freundlich’s models have been used for the same adsorbate (nickel ion) and adsorbent (granular activated carbon) in the literature [22].

The dimensionless factor of separation in the Langmuir model based on C'_0 as the maximum initial metal concentration is introduced as follows:

$$R_L = \frac{1}{1 + bC'_0} \quad (14)$$

where R_L determines the adsorption situation which is unfavorable if $R_L > 1$, linear if $R_L = 1$, irreversible if $R_L = 0$,

and favorable if $0 < R_L < 1$ [26]. According to Table 2, for Ni removal $R_L = 0.456$ and thus, the adsorption of Ni is favorable. Also, $q_m = 3.28$ mg/g in Table 2 is obtained as the maximum capacity of adsorption of activated carbon for nickel removal.

In D–R equation, for determining the adsorption type E_s parameter can be defined as follows:

$$E_s = \frac{1}{(2K_D)^{0.5}} \quad (15)$$

Given $E_s = 0.29$ (kJ/mol) obtained in this work, physical adsorption is predominant (as this is less than 8 kJ/mol) [31].

Finally, based on the plot of Eq. (11), the enthalpy and entropy of adsorption are determined. These values are presented in Table 3. Negative Gibbs free energies in Table 3 suggest that Ni adsorption is feasible. Also, the

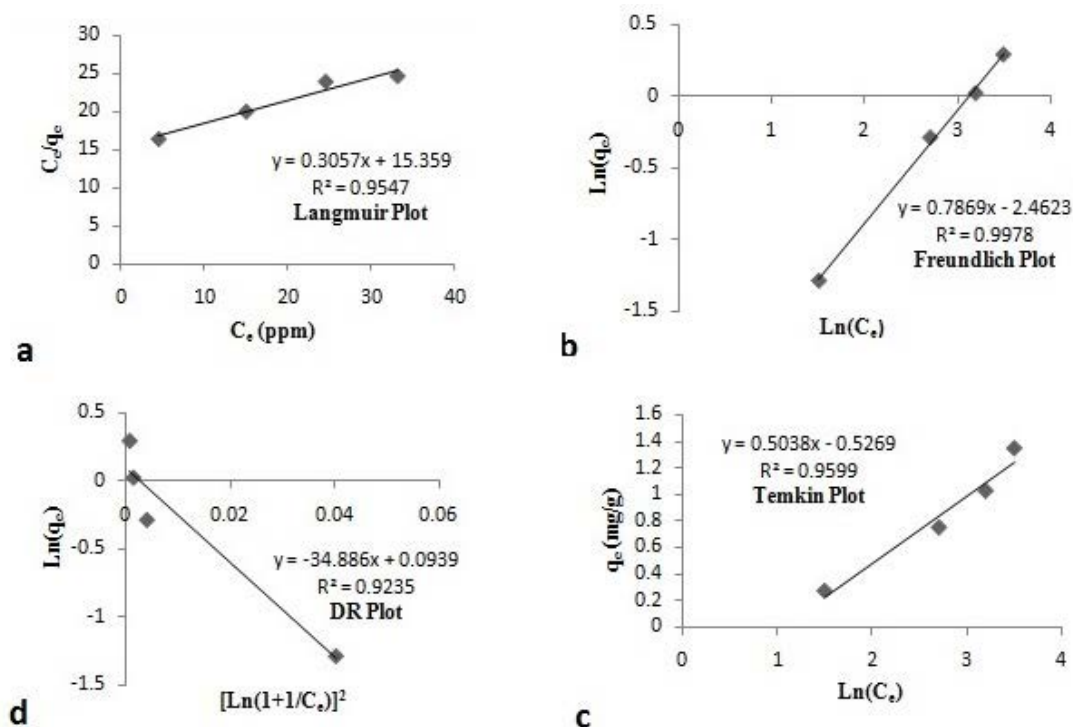


Fig. 4. Equilibrium plots for Ni removal, Langmuir (a), Freundlich (b), Temkin (c), and Dubinin–Radushkevich (d).

Table 1
Kinetic constants for Ni removal

Kinetic of adsorption mechanisms		
Pseudo-first-order	k_1 (1/min)	0.009
	R^2	0.96
Pseudo-second-order	k_2 (g/mg min)	0.15
	R^2	0.998
Elovich	b (g/mg)	11.623
	a (mg/g min)	839.359
	R^2	0.901
	Mass transfer mechanisms	
Intraparticle diffusion	C (mg/g)	0.934
	K_{int} (mg/g min ^{0.5})	0.026
Weber and Morris	R^2	0.951
	B (1/min)	0.0152
Boyd's model	R^2	0.83

positive enthalpy values show an endothermic process, and positive entropy values indicate the affinity of activated carbon for nickel removal. These signs are similar to previous literature data [28].

3.2. Nickel ion experimental design

In this work, Box–Behnken design (BBD) type of RSM was applied, as BBD needs fewer experiments for optimization vs. central composite design type. Also, BBD type RSM

Table 2
Equilibrium constants for Ni removal

Langmuir constants	q_m (mg/g)	3.279
	b (L/mg)	0.0199
	R_L	0.456
Freundlich constants	R^2	0.954
	K_f (mg/g)	0.085
	n	1.272
D–R constants	R^2	0.998
	q_m (mg/g)	1.097
	K_D (mol ² /kJ ²)	5.878
Temkin constants	E_s (kJ/mol)	0.292
	R^2	0.923
	B_b (J/mol)	4843
	A_a (L/mg)	0.351
	R^2	0.959

has been used in a recent experimental design literature work successfully [32].

The operating conditions of the experimental design for the nickel removal are adjusted within the range of carbon mass (A : 1–3 g/100 mL), pH (B : 2–6), and initial Ni concentration (C : 10–50 mg/L). The responses, as nickel removal efficiencies, are presented in Table 4. This table shows twelve various tests and five center points. Analysis of variance (ANOVA) and brief statistical results for nickel removal are presented in Tables 5 and 6, respectively.

The RSM suggested correlation for Ni removal is as follows:

Table 3
Estimation of enthalpy and entropy of adsorption

<i>T</i> (K)	ΔG° (kJ/mol)	ΔS° (J/(mol K))	ΔH° (kJ/mol)
301	-2.32		
316	-3.43	60.06	15.71
326	-3.78		

$$y = 61.45 + 11.08A + 15.94B - 2.58C + 3.74AB + 0.25AC - 0.7BC - 3.36A^2 - 20.51B^2 - 5.14C^2 \quad (16)$$

The Eq. (16) in decoded variables is presented as:

$$y = 61.45 + 11.08m + 15.94p - 2.58c + 3.74mp + 0.25mc - 0.7pc - 3.36m^2 - 20.51p^2 - 5.14c^2 \quad (17)$$

where *m* is mass of carbon (g) per 100 mL solution, *p* denotes the pH of the solution, and *c* shows the initial Ni concentration (mg/L).

RSM method accuracy is characterized by a high *F*-value and low *p*-values (less than 0.05) in ANOVA results. For Ni adsorption, Table 5 shows *F* = 65.01, which verifies that the noise is negligible. Furthermore, the low probability (*p* < 0.0001) in Table 5 suggests that the above-correlated equation is significant. In this work, *A*, *B*, *C*, *AB*, *B*² and *C*² have been significant in Eq. (16) for Ni adsorption. Also, "predicted *R*²" equal to 0.854 is relatively compatible with "adjusted *R*²" of 0.973. Further, "adequacy precision" or the signal-to-noise ratio should be higher than 4. The ratio of 23.73 in this study indicates a high value of the signal,

thus demonstrating that the suggested correlation is applicable for design purposes.

One of the optimum conditions for maximum Ni adsorption was determined by RSM software as 73.0% at pH = 5.14, 2.98 g carbon/100 mL solution, and 33.26 mg/L initial nickel concentration. Experimental Ni removal efficiency for this validation test was obtained as 73.33%, which shows very good accuracy. However, the remaining nickel concentration after adsorption treatment is still high. Thus, modification of the activated carbon has been proposed in this work for reducing the remaining nickel concentration, which will be explained in section 3.3 (tests by carbon after modification).

The normal probability plot and internally studentized residuals for Ni removal are illustrated in Figs. 5a and b. Since a close agreement is seen between the points and the related line in Fig. 5a, thus the model is validated. Meanwhile, the comparison between experimental and predicted values is obtained with good accuracy. Finally, the residuals vs. predicted values are shown in Fig. 5b. High dispersion of the points in this figure verifies the RSM model consistency.

Now, the quantitative effects of operating variables are predicted by the RSM model. The effects of carbon/water ratio, pH of the solution, and initial Ni concentration on Ni the removal efficiency are indicated in Fig. 6a. According to this figure, it is clear that nickel removal has improved by increasing the carbon/water ratio with a mild slope. Further, upon elevation of pH from 2 to about 5, the removal efficiency has grown dramatically, after which it decreased between pH 5 to 6. Thus, pH 5.1 is the best for nickel removal which is in close agreement with previous reports [33]. Finally, the influence of variations of the initial nickel concentration on the nickel removal

Table 4
RSM responses as nickel removal efficiencies

Standard order	Run	A: mass/100 mL (g)	B: pH	C: concentration (mg/L)	Ni removal (%)	
					Actual value	Predicted value
1	5	1	2	30	13.33	14.29
2	3	3	2	30	26.67	29.03
3	6	1	6	30	41	38.69
4	16	3	6	30	69.3	68.39
5	15	1	4	10	42.4	44.71
6	17	3	4	10	65.4	66.41
7	9	1	4	50	40	38.91
8	7	3	4	50	64	61.65
9	2	2	2	10	25	21.78
10	12	2	6	10	55	55.02
11	4	2	2	50	18	17.86
12	11	2	6	50	45.2	48.38
13	1	2	4	30	63.25	61.48
14	8	2	4	30	63.24	61.48
15	10	2	4	30	58.53	61.48
16	13	2	4	30	60.7	61.48
17	14	2	4	30	61.54	61.48

Table 5
Analysis of ANOVA for nickel removal

Source	Sum of squares	Degree of freedom	Mean square	F-value ^a	p-value (Prob. > F) ^b	
Model	5,157.55	9.0	573.06	65.01	<0.0001 ^s	Significant
A: mass/100 mL	982.13	1.0	982.13	111.41	<0.0001 ^s	
B: pH	2,032.03	1.0	2,032.03	230.51	<0.0001 ^s	
C: concentration	53.05	1.0	53.05	6.02	0.0439 ^s	
AB	55.95	1.0	55.95	6.35	0.0399 ^s	
AC	0.25	1.0	0.25	0.028	0.871 ⁿ	
BC	1.96	1.0	1.96	0.22	0.6516 ⁿ	
A ²	47.63	1.0	47.63	5.4	0.053 ⁿ	
B ²	1,771.8	1.0	1,771.8	200.99	<0.0001 ^s	
C ²	111.18	1.0	111.18	12.61	0.0093 ^s	
Residual	61.71	7.0	8.82			
Lack of fit	46.17	3.0	15.39	3.96	0.1084 ⁿ	Not significant
Pure error	15.54	4.0	3.89			
Corr. total	5,219.25	16.0				

^aTest for comparing the model with residual (error) variance;

^bProbability of finding the observed F-value when the null hypothesis is true;

^sSignificant at $p < 0.05$;

ⁿNot significant at $p > 0.05$.

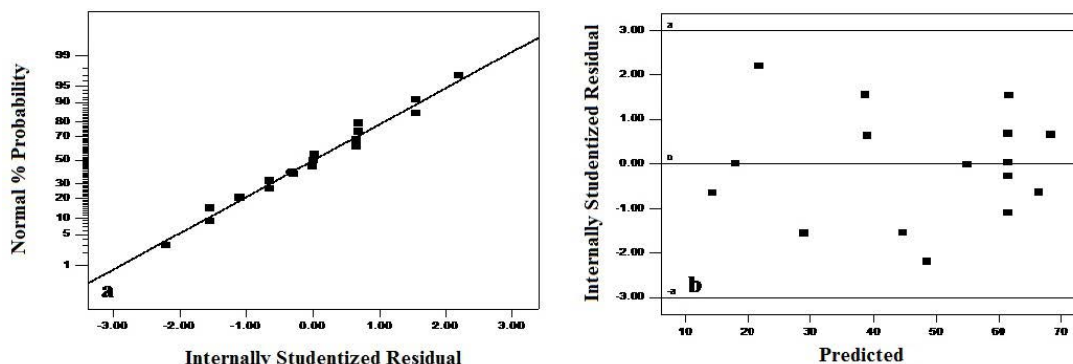


Fig. 5. Normal probability plot of residuals for Ni removal in RSM (a), and internally studentized residuals vs. predicted values from RSM (b).

Table 6
Brief statistical study for nickel removal

Standard deviation	2.97	R-squared	0.9882
Mean	47.8	Adj. R-squared	0.9730
C.V. %	6.21	Pred. R-squared	0.8538
PRESS	762.96	Adeq. precision	23.729

efficiency is small. Three-dimensional plots for binary interactions in the Ni adsorption by activated carbon are illustrated in Fig. 6b. Based on this figure, changes in two important parameters (mass of carbon and pH) lead to more variations in the three-dimensional removal efficiency curve as compared to a less important parameter (concentration).

3.3. Tests by carbon after modification

PSD development of activated carbon vs. time of gasification has been reported in the literature [25]. Based on this idea, here the PSD of activated carbon was modified through CO₂ gasification for improving the mesopore fraction and enhancing Ni removal.

The gasification was accomplished under two mild and severe operating conditions. The operating conditions of these two gasification experiments are reported in Table 7. The average outlet CO/CO₂ mole fraction ratios from the reactor was measured by a mass spectrometer as 0.7/0.3 and 0.64/0.36 for mild and severe conditions, respectively. The weight losses after the gasification were determined as 15% and 22% for mild and severe conditions, respectively.

The PSDs of initial and modified activated carbons are presented in Fig. 7. Based on this figure, BET surface areas,

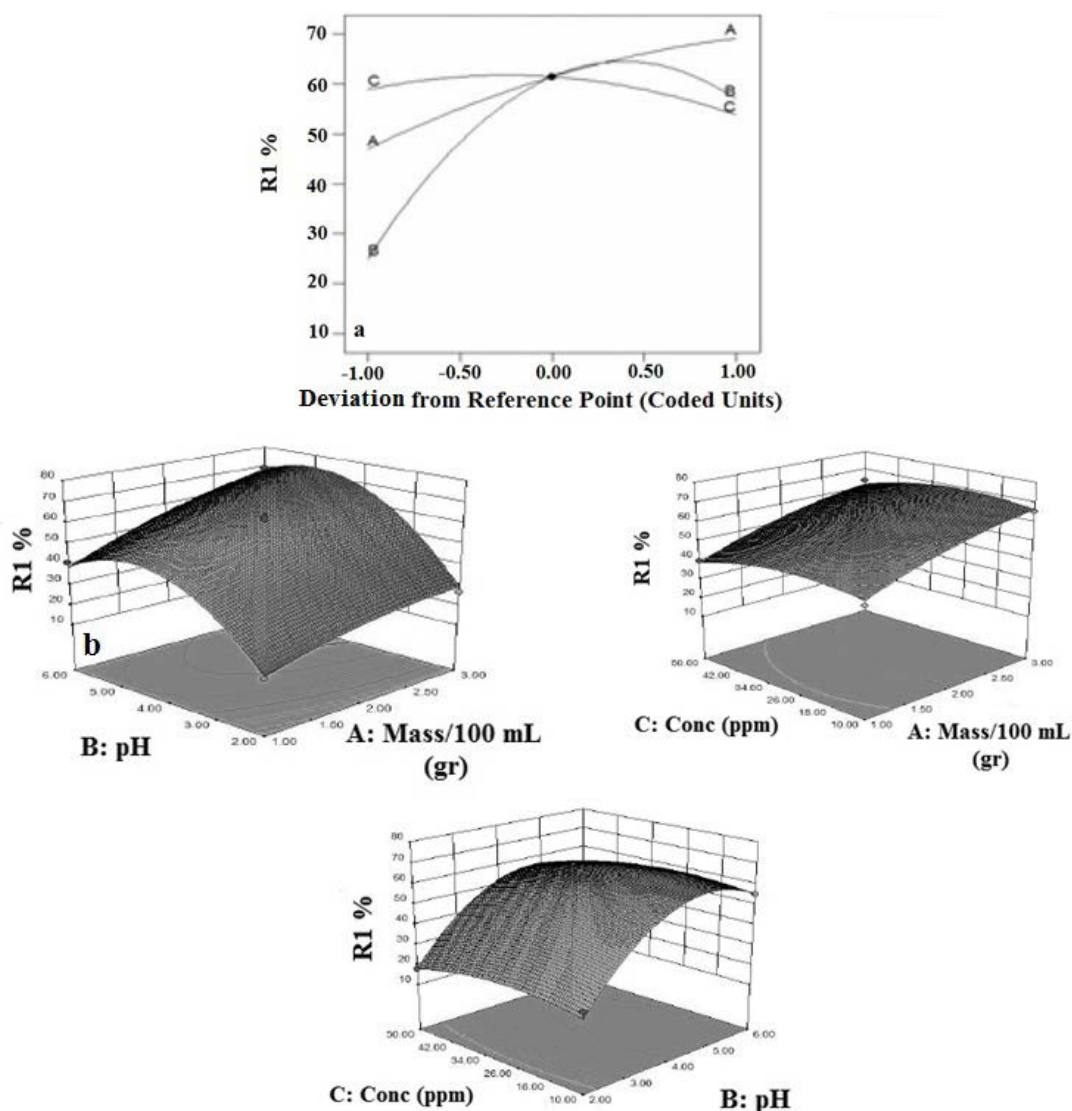


Fig. 6. Effect of carbon/water ratio, pH, and concentration in Ni removal by RSM (a), and three-dimensional binary interaction plots for Ni removal from RSM (b).

Table 7
Operating conditions of two kinds of CO₂ gasification

Kind of gasification	Time (min)	CO ₂ stream (mL/min)	Temperature (°C)	Initial mass (g)
Mild	75	450	900	100
Severe	90	550	950	60

SF method micropore volumes, and BJH method mesopore volumes were obtained, as presented in Table 8.

According to Table 8, in mild gasification, the pores enlarge and the mesopore volume increases considerably thereby reducing the BET surface area. Meanwhile, a small amount of new micropores appears in the carbon structure. Note that micropores diminish with respect to the initial

carbon, mesopores increase to a little extent, and probably some macro-pores are produced after the severe gasification. An experimental activation work reported that the maximum surface area was obtained at about 54% burn-off [34]. Higher activation over this point led to the destruction of mesopores and the formation of some macro-pores (overlapping mesopores during their growth), which reduced the BET surface area [34].

Further, the pH of zero charge points of various adsorbents are also expressed in Table 8. As these values show, there is no significant difference between the pH of zero charge points of initial and modified activated carbons.

FTIR spectrum of these adsorbents are presented in Fig. 8. As this figure indicates, FTIR peaks of the initial and modified activated carbons are nearly identical. The absorption peaks at about 3,400 cm⁻¹ can be assigned to moisture, and peaks near 1,100 cm⁻¹ can be attributed to the stretching

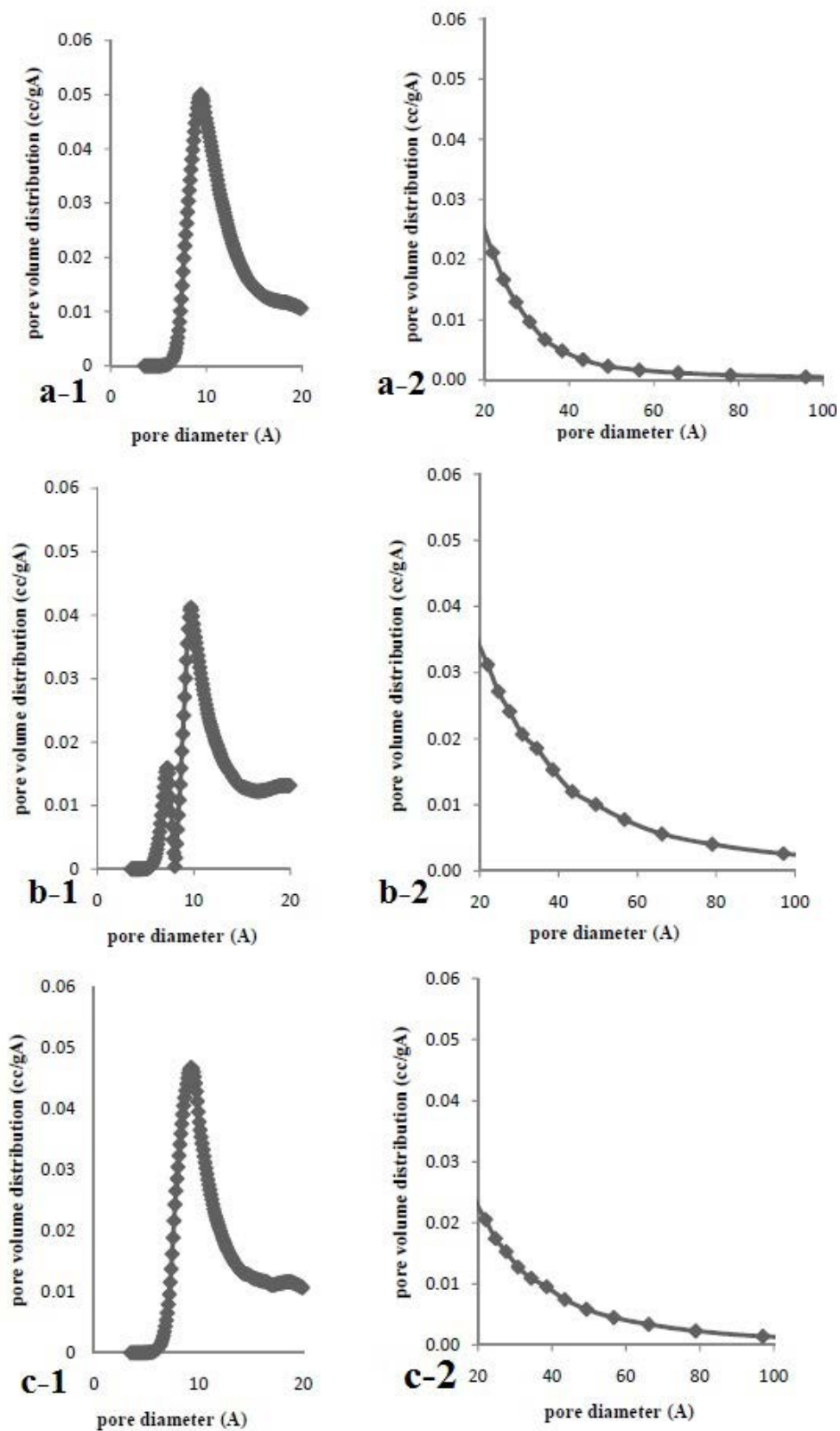


Fig. 7. Micro (SF) PSDs (1), and meso (BJH) PSDs (2), of the initial (a), and modified activated carbons by CO₂ gasification at 900°C (b), and at 950°C (c).

Table 8
BET surface areas, SF micropore volumes, BJH mesopore volumes, and pH of zero charge point for initial and modified activated carbons

Kind of activated carbon	BET surface area (m ² /g)	SF method micropore volume (mL/g)	BJH method mesopore volume (mL/g)	pH of zero charge point
Initial activated carbon	1,064	0.496	1.36	9.58
Modified carbon under the mild condition	800	0.537	1.71	9.68
Modified carbon under the severe condition	772	0.477	1.47	9.95

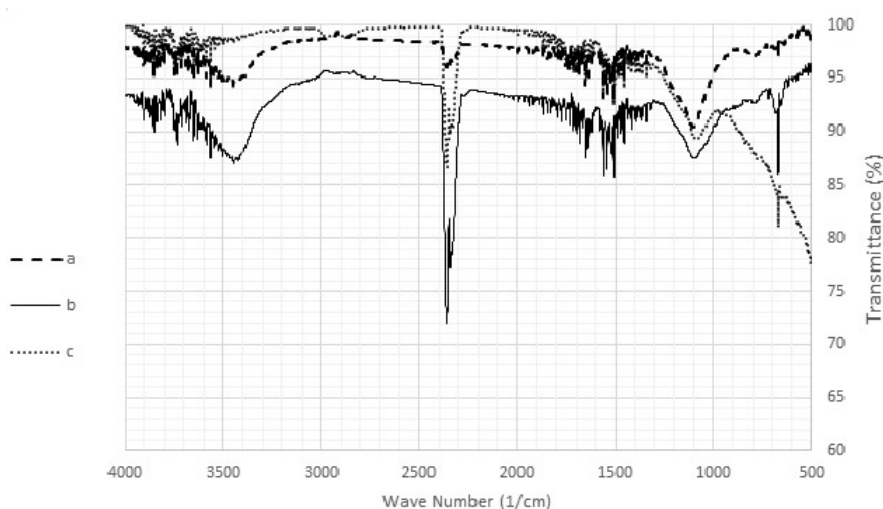


Fig. 8. FTIR spectrum of initial carbon (a), modified carbon at mild condition (b), and modified carbon at severe condition (c).

vibration of C–OH. Finally, peaks at about 2,300 cm⁻¹ in the modified activated carbons are probably due to CO₂ trapped in the pores.

SEM graphs of the initial and modified activated carbons are illustrated in Fig. 9. As this figure shows, it seems that some smaller pores have developed in the modified activated carbons vs. initial carbon. However, the destruction of the porous structure has appeared in the modified activated carbon from severe CO₂ gasification conditions (Fig. 9c).

A typical blank Ni removal test was performed through the initial carbon at 2 g carbon/100 mL solution, pH = 4, and 30 mg/L initial concentration, which showed 63.25% removal efficiency. At the same time, Ni removal efficiencies for adsorption by the modified activated carbons under the mild and severe gasification conditions were determined as 83.6% and 71.7%, respectively. Thus, modification by CO₂ gasification can enhance the Ni removal performance considerably, even under this blank (non-optimized) condition. Nevertheless, the mild gasification condition is a better case for Ni removal. Meanwhile, it seems that enlarged pore diameters under the severe gasification condition are greatly larger than the nickel ion size. Finally, the Ni removal efficiency by this modified carbon (in the mild gasification) under the optimum RSM condition improved from 73.33% (of initial carbon) to 96.12%.

3.4. Regeneration of the consumed adsorbent

The regeneration tests were accomplished via H₂SO₄, HNO₃, and electro-kinetic method, where the obtained desorption efficiencies were compared through distilled water regeneration (with adequate agitation) test.

Ni regeneration efficiency after 6 h in distilled water was only 7.1%. The regeneration efficiency for the best electro-kinetic test in water (at 0.5 A, 12 V, and 3 h) was obtained as 20%. This relatively low value is probably due to the elevation of pH at cathode and precipitation of the metal ion.

On the other hand, Ni desorption by sulfuric acid and nitric acid was relatively successful. In this case, an adsorption test was performed initially under the optimum RSM conditions. Further, saturated carbon was separated from the solution and dried in an oven. Then, the regeneration test was accomplished with the same ratio of carbon/acid solution.

The results of H₂SO₄ and HNO₃ desorption at various concentrations are illustrated in Fig. 10a. Further, the results of H₂SO₄ and HNO₃ regeneration at various times are presented in Fig. 10b. As this figure indicates, the best Ni regeneration efficiency was obtained as 78.4% for 0.5 M HNO₃ at 6 h, while the best regeneration by H₂SO₄ was about 65%.

Finally, the electro-kinetic tests were conducted in sulfuric acid, where the obtained results were excellent and

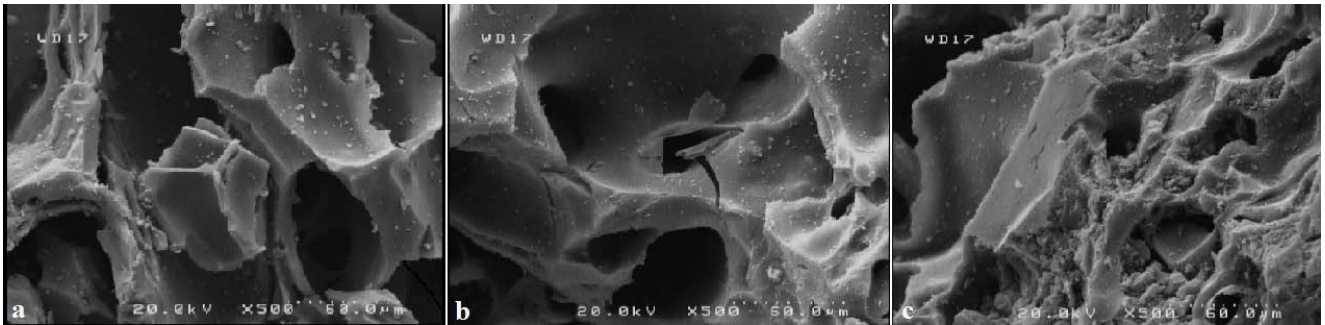


Fig. 9. SEM graphs of initial carbon (a), modified carbon at mild condition (b), and modified carbon at severe condition (c) with 500× magnification.

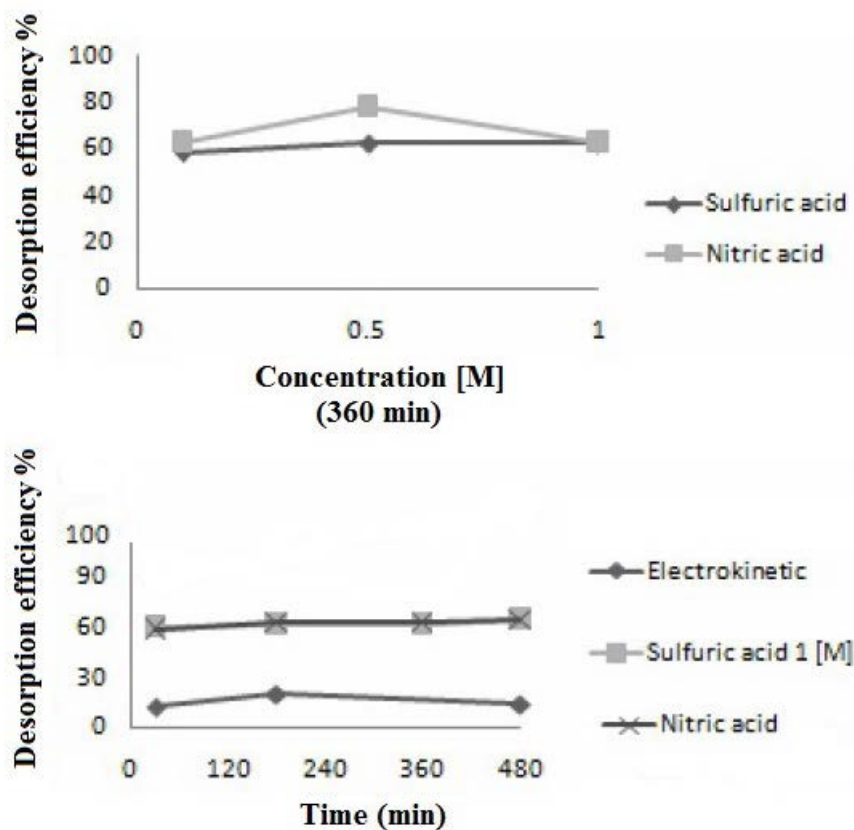


Fig. 10. Regeneration efficiencies vs. concentration by sulfuric acid and nitric acid (a), and desorption efficiencies vs. time for the electro-kinetic, 1 M sulfuric acid, and 1 M nitric acid (b).

desorption efficiencies near 100% were obtained within a short time. A similar result (regeneration efficiency near 100% in some cases) has been reported in the literature for a biomass-based activated carbon [35].

4. Conclusion

In this study, the removal of nickel ion was tested by activated carbon in an aqueous solution for understanding the governing kinetics, equilibrium, and thermodynamic equations. Then, the experimental design RSM method was also studied. In this regard, the effects of

operating parameters (pH, carbon/liquid ratio, and initial Ni concentration) were considered on the adsorption efficiencies. Further, CO₂ gasification was used for modifying the PSD of the commercial activated carbon. Finally, various regeneration methods were performed for the consumed carbon.

The main results obtained from this work are summarized as follows:

- The appropriate kinetic model for nickel adsorption was pseudo-second-order.
- For the equilibrium section, the Freundlich equation was the best for nickel removal.

- Since the related n was near one, thus Langmuir equation can also be applied.
- Ni adsorption was found as endothermic and spontaneous.
- The effects of increasing the pH and carbon/liquid ratio were positive.
- The optimum condition for Ni removal was determined by RSM as pH = 5.14, 2.98 g carbon/100 mL solution, and 33.26 mg/L initial Ni concentration.
- The maximum Ni adsorption efficiency was predicted as 73.0%, while the validation test showed 73.3% removal ($q_{\max} = 3.28$ mg/g) with an excellent agreement.
- A similar study in the literature showed $q_{\max} = 2.87$ mg/g for another type of granular activated carbon [23].
- Modification of PSD through CO₂ gasification was successful, due to the domination of the mesopore volumes.
- Nickel removal efficiency by this modified carbon under one of the optimum conditions improved by 31.1% in relation to the initial adsorbent.
- The complete regeneration of the spent activated carbon was obtained through the electro-kinetic test in the presence of sulfuric acid.

References

- [1] J. Anandkumar, B. Mandal, Removal of Cr(VI) from aqueous solution using Bael fruit (*Aegle marmelos correa*) shell as an adsorbent, *J. Hazard. Mater.*, 168 (2009) 633–640.
- [2] H. Kalavathy, B. Karthik, L.R. Miranda, Removal and recovery of Ni and Zn from aqueous solution using activated carbon from *Hevea brasiliensis*: batch and column studies, *Colloids Surf., B*, 78 (2010) 291–302.
- [3] EPA, National Primary Drinking Water Regulations for Nickel, United States Environmental Protection Agency, United States, 1995.
- [4] F.L. Fu, Q. Wang, Removal of heavy metal ions from wastewaters: a review, *J. Environ. Manage.*, 92 (2011) 407–418.
- [5] Ç. Kırbıyık, A.E. Pütün, E. Pütün, Comparative studies on adsorptive removal of heavy metal ions by biosorbent, bio-char and activated carbon obtained from low cost agro-residue, *Water Sci. Technol.*, 73 (2016) 423–436.
- [6] T. Tay, M. Candan, M. Erdem, Y. Çimen, H. Türk, Biosorption of cadmium ions from aqueous solution onto non-living lichen *Ramalina fraxinea* biomass, *CLEAN Soil Air Water*, 37 (2009) 249–255.
- [7] M. Kavand, T. Kaghazchi, M. Soleimani, Optimization of parameters for competitive adsorption of heavy metal ions (Pb²⁺, Ni²⁺, Cd²⁺) onto activated carbon, *Korean J. Chem. Eng.*, 31 (2014) 692–700.
- [8] M. Danish, R. Hashim, M. Rafatullah, O. Sulaiman, A. Ahmad, Govind, Adsorption of Pb(II) ions from aqueous solutions by date bead carbon activated with ZnCl₂, *CLEAN Soil Air Water*, 39 (2011) 392–399.
- [9] T. Altun, E. Pehlivan, Removal of copper(II) ions from aqueous solutions by walnut-, hazelnut- and almond shells, *CLEAN Soil Air Water*, 35 (2007) 601–606.
- [10] K.L. Wasewar, M. Atif, B. Prasad, I.M. Mishra, Adsorption of zinc using tea factory waste: kinetics, equilibrium and thermodynamics, *CLEAN Soil Air Water*, 36 (2008) 320–329.
- [11] D. Waseem, T. Ebadi, A. Fahimifar, Optimization of hexavalent chromium removal from aqueous solution using acid-modified granular activated carbon as adsorbent through response surface methodology, *Korean J. Chem. Eng.*, 32 (2015) 1119–1128.
- [12] M. Danish, R. Hashim, M.N.M. Ibrahim, M. Rafatullah, O. Sulaiman, Surface characterization and competitive adsorption properties of Cr(VI) on pyrolysed adsorbents of *Acacia mangium* wood and *Phoenix dactylifera L.* stone carbon, *J. Anal. Appl. Pyrolysis*, 97 (2012) 19–28.
- [13] M.N. Siddiqui, H.H. Redhwi, A.A. Al-Saadi, M. Rajeh, T.A. Saleh, Kinetic and computational evaluation of activated carbon produced from rubber tires toward the adsorption of nickel in aqueous solutions, *Desal. Water Treat.*, 57 (2016) 17570–17578.
- [14] A. Damaj, G.M. Ayoub, M. Al-Hindi, H. El Rassy, Activated carbon prepared from crushed pine needles used for the removal of Ni and Cd, *Desal. Water Treat.*, 53 (2015) 3371–3380.
- [15] M. Ugurlu, I. Kula, M.H. Karaoglu, Y. Arslan, Removal of Ni(II) ions from aqueous solutions using activated-carbon prepared from olive stone by ZnCl₂ activation, *Environ. Prog. Sustainable Energy*, 28 (2009) 547–557.
- [16] H. Hasar, Adsorption of nickel(II) from aqueous solution onto activated carbon prepared from almond husk, *J. Hazard. Mater.*, 97 (2003) 49–57.
- [17] M. Arshadi, M.J. Amiri, S. Mousavi, Kinetic, equilibrium and thermodynamic investigations of Ni(II), Cd(II), Cu(II) and Co(II) adsorption on barley straw ash, *Water Resour. Ind.*, 6 (2014) 1–17.
- [18] M. Amini, H. Younesi, Biosorption of Cd(II), Ni(II) and Pb(II) from aqueous solution by dried biomass of *Aspergillus niger*: application of response surface methodology to the optimization of process parameters, *CLEAN Soil Air Water*, 37 (2009) 776–786.
- [19] M. Danish, R. Hashim, M.N.M. Ibrahim, M. Rafatullah, O. Sulaiman, T. Ahmad, M. Shamsuzzoha, A. Ahmad, Sorption of copper(II) and nickel(II) ions from aqueous solutions using calcium oxide activated date (*Phoenix dactylifera*) stone carbon: equilibrium, kinetic, and thermodynamic studies, *J. Chem. Eng. Data*, 56 (2011) 3607–3619.
- [20] M. Karnib, A. Kabbani, H. Holail, Z. Olama, Heavy metals removal using activated carbon, silica and silica activated carbon composite, *Energy Procedia*, 50 (2014) 113–120.
- [21] K. Kadirvelu, C. Faur-Brasquet, P. Le Cloirec, Removal of Cu(II), Pb(II), and Ni(II) by adsorption onto activated carbon cloths, *Langmuir*, 16 (2000) 8404–8409.
- [22] C.Y. Lu, C. Liu, G.P. Rao, Comparisons of sorbent cost for the removal of Ni²⁺ from aqueous solution by carbon nanotubes and granular activated carbon, *J. Hazard. Mater.*, 151 (2008) 239–246.
- [23] D. Satapathy, G.S. Natarajan, Potassium bromate modification of the granular activated carbon and its effect on nickel adsorption, *Adsorption*, 12 (2006) 147–154.
- [24] H. Marsh, F.R. Reinoso, *Activated Carbon*, Elsevier Science and Technology Books, London, 2006.
- [25] A.H. Faramarzi, T. Kaghazchi, H. Ale Ebrahim, A. Afshar Ebrahimi, A mathematical model for prediction of pore size distribution development during activated carbon preparation, *Chem. Eng. Commun.*, 202 (2015) 131–143.
- [26] R.M. Ali, H.A. Hamad, M.M. Hussein, G.F. Malash, Potential of using green adsorbent of heavy metal removal from aqueous solutions: adsorption kinetics, isotherm, thermodynamic, mechanism and economic analysis, *Ecol. Eng.*, 91 (2016) 317–332.
- [27] D.D. Do, *Adsorption Analysis: Equilibria and Kinetics*, Imperial College Press, London, 1998.
- [28] F. Bouhamed, Z. Elouear, J. Bouzid, B. Ouddane, Multi-component adsorption of copper, nickel and zinc from aqueous solutions onto activated carbon prepared from date stones, *Environ. Sci. Pollut. Res.*, 23 (2016) 15801–15806.
- [29] M.A. Ale Ebrahim, T. Ebadi, Zinc and nickel removal from aqueous solution by activated carbon in batch and permeable reactive barrier (PRB) systems, *Desal. Water Treat.*, 118 (2018) 181–194.
- [30] N. Balasubramanian, T. Kojima, C. Srinivasakannan, Arsenic removal through electrocoagulation: kinetic and statistical modeling, *Chem. Eng. J.*, 155 (2009) 76–82.
- [31] A. Sari, M. Tuzen, D. Citak, M. Soylak, Equilibrium, kinetic and thermodynamic studies of adsorption of Pb(II) from aqueous solution onto Turkish kaolinite clay, *J. Hazard. Mater.*, 149 (2007) 283–291.
- [32] R. Kumar, R. Singh, N. Kumar, K. Bishnoi, N.R. Bishnoi, Response surface methodology approach for optimization of biosorption process for removal of Cr(VI), Ni(II) and Zn(II)

- ions by immobilized bacterial biomass sp. *Bacillus brevis*, *Chem. Eng. J.*, 146 (2009) 401–407.
- [33] R.C. Bansal, M. Goyal, *Activated Carbon Adsorption*, Taylor & Francis, London, 2005.
- [34] M. Asadullah, M.A. Rahman, M.A. Motin, M.B. Sultan, Preparation and adsorption studies of high specific surface area activated carbons obtained from the chemical activation of jute stick, *Adsorpt. Sci. Technol.*, 24 (2006) 761–770.
- [35] H. Runtti, S. Tuomikoski, T. Kangas, U. Lassi, T. Kuokkanen, J. Rämö, Chemically activated carbon residue from biomass gasification as a sorbent for iron(II), copper(II) and nickel(II) ions, *J. Water Process Eng.*, 4 (2014) 12–24.